Increased Expression of Insulin-like Growth Factor-II Messenger RNA–Binding Protein 1 Is Associated with Tumor Progression in Patients with Lung Cancer

Tatsuya Kato,[1,2] Satoshi Hayama,[1] Takumi Yamabuki,[1] Nobuhisa Ishikawa,[1] Masaki Miyamoto,[2] Tomoo Ito,[3] Eiju Tsuchiya,[4] Satoshi Kondo,[2] Yusuke Nakamura,[1] and Yataro Daigo[1]

Abstract

Purpose: To identify novel biomarkers and therapeutic targets for lung cancers, we screened for genes that were highly transactivated in a large proportion of non–small cell lung cancers (NSCLC) using a cDNA microarray representing 27,648 genes.

Experimental Design: A gene encoding insulin-like growth factor-II mRNA-binding protein 1 (IMP-1) was selected as a candidate (≥3-fold expression than in normal lung tissue in about 70% of NSCLCs). Tumor tissue microarray was applied to examine expression of IMP-1 protein in archival lung cancer samples from 267 patients and investigated its clinicopathologic significance. A role of IMP-1 in cancer cell growth and/or survival was examined by small interfering RNA experiments. Cellular invasive activity of IMP-1 on mammalian cells was examined using Matrigel assays. mRNAs associated with IMP-1 in cancer cells were also isolated by RNA immunoprecipitation followed by cDNA microarray analysis.

Results: Positive immunostaining of IMP-1 was correlated with male ($P = 0.0001$), tumor size ($P = 0.0003$), non-adenocarcinoma histology ($P < 0.0001$), smoking history ($P = 0.0005$), non–well-differentiated tumor grade ($P = 0.0001$), and poor prognosis ($P = 0.0053$). Suppression of IMP-1 expression with small interfering RNA effectively suppressed growth of NSCLC cells. In addition, we identified that exogenous expression of IMP-1 increased the migratory activity of mammalian cells. IMP-1 was able to bind to mRNAs encoding a variety of proteins involved in signal transduction, cell cycle progression, cell adhesion and cytoskeleton, and various types of enzymatic activities.

Conclusions: These results suggest that IMP-1 expression is likely to play important roles in lung cancer development and progression, and that IMP-1 is a prognostic biomarker and a promising therapeutic target for lung cancer.

Lung cancer is one of the most common causes of cancer death worldwide, and non–small cell lung cancer (NSCLC) accounts for nearly 80% of those cases (1). Many genetic alterations involved in development and progression of lung cancer have been reported, but the precise molecular mechanisms remain unclear (2). Over the last decade, newly developed cytotoxic agents, including paclitaxel, docetaxel, gemcitabine, and vinorelbine, have emerged to offer multiple therapeutic choices for patients with advanced NSCLC. However, those regimens provide only limited survival benefits compared with cisplatin-based therapies (3, 4). Recently, new agents targeting the epidermal growth factor receptor pathway, erlotinib (Tarceva, OSI Pharmaceuticals, Melville, NY) and gefitinib (Iressa, AstraZeneca, Wilmington, DE), were developed and were shown to be very effective for a subset of NSCLC patients. However, even if all kinds of available treatments are applied, the proportion of patients showing good response is still very limited (5–8). Hence, new therapeutic strategies are eagerly awaited.

Systematic analysis of expression levels of thousands of genes using cDNA microarray is an effective approach to identify molecules involved in carcinogenic pathways that can be candidates for development of novel therapeutics and diagnostics. We have been attempting to isolate potential molecular targets for diagnosis and/or treatment of lung cancer by analyzing genome-wide expression profiles of various types of lung cancer cells on a cDNA microarray containing 27,648 genes, using tumor cell populations purified by laser-capture microdissection (9–11). To verify the biological and clinicopathologic significance of the respective gene products, we have

Authors' Affiliations: [1]Laboratory of Molecular Medicine, Human Genome Center, Institute of Medical Science, The University of Tokyo, Tokyo, Japan; Departments of [2]Surgical Oncology and [3]Surgical Pathology, Hokkaido University Graduate School of Medicine, Sapporo, Japan; and [4]Kanagawa Cancer Center Research Institute, Kanagawa, Japan

Received 5/30/06; revised 9/26/06; accepted 9/27/06.

The costs of publication of this article were defrayed in part by the payment of page charges. This article must therefore be hereby marked *advertisement* in accordance with 18 U.S.C. Section 1734 solely to indicate this fact.

Note: Supplementary data for this article are available at Clinical Cancer Research Online (http://clincancerres.aacrjournals.org/).

T. Kato and S. Hayama contributed equally to this work.

Requests for reprints: Yataro Daigo, Laboratory of Molecular Medicine, Human Genome Center, Institute of Medical Science, The University of Tokyo, 4-6-1 Shirokanedai, Minato-ku, Tokyo 108-8639, Japan. Phone: 81-3-5449-5457; Fax: 81-3-5449-5406; E-mail: ydaigo@ims.u-tokyo.ac.jp.

doi:10.1158/1078-0432.CCR-06-1297

also been performing tumor tissue microarray analysis of clinical lung cancer specimens (12–15). This systematic approach revealed that insulin-like growth factor-II (IGF-II) mRNA-binding protein 1 (IMP-1; alias CRDBP, c-*myc* coding region determinant binding protein) was frequently overexpressed in primary NSCLCs.

IMP-1 is a member of the zipcode-binding protein family, which are orthologous and paralogous members of the same vertebrate RNA-binding protein family, consisting of two RNA recognition motifs and four K homology domains (16). IMP-1 is expressed in most embryonic tissues. Analysis of total RNA from mouse embryos indicated a peak of IMP-1 expression at embryonic day 12.5 followed by decline toward birth and its disappearance in neonatal mice shortly after birth (17). IMP-1 was overexpressed in several human cancers and has been suggested to play various roles in determining the posttranscriptional fate of its RNA targets and to act as a nucleocytoplasmic shuttling protein exhibiting a distinct pattern of localization in the cytoplasm (16, 18–23). The protein is distributed along with microtubules and is likely to be transported toward the leading edge in motile cells. Its nuclear export and cytoplasmic movement depend on RNA binding, implying that IMP-1 recognizes its targets in the nucleus and thereby defines their cytoplasmic fate. IMP-1 was indicated to play a significant role in polarizing genetic information by defining cytoplasmic RNA localization, a critical mechanism especially in developmental systems for the generation of subcellular asymmetries in protein abundance. H19 RNA colocalizes with IMP-1, and removal of the high-affinity attachment site led to delocalization of the truncated RNA (23), indicating that IMP-1 are involved in cytoplasmic trafficking of mRNA (22).

We here report the identification of IMP-1 as a novel prognostic marker and a potential target for therapeutic agents and also provide evidence for its possible role in human pulmonary carcinogenesis through its binding to various mRNAs that encode proteins related with cell proliferation and invasion.

Materials and Methods

Lung cancer cell lines and clinical samples. The human lung cancer lines used in this study were as follows: A427, A549, LC319, PC3, PC9, PC14, and NCI-H1373 (adenocarcinomas); NCI-H1666 and NCI-H1781 (bronchioloalveolar carcinomas); NCI-H226 and NCI-H647 (adenosquamous carcinomas); RERF-LC-AI, SK-MES-1, EBC-1, LU61, NCI-H520, NCI-H1703, and NCI-H2170 (lung squamous cell carcinomas); LX1 (lung large cell carcinoma); DMS114, DMS273, SBC-3, and SBC-5 (SCLC). All cells were grown in monolayer in appropriate medium supplemented with 10% FCS and were maintained at 37°C in atmospheres of humidified air with 5% CO_2. Human small airway epithelial cells were grown in optimized medium (SAGM) purchased from Cambrex Bioscience, Inc. (Walkersville, MD). Fourteen primary NSCLCs (7 adenocarcinomas and 7 squamous cell carcinomas) were obtained along with adjacent normal lung tissue samples from patients undergoing surgery at Hokkaido University and its affiliated hospitals (Sapporo, Japan).

A total of 267 formalin-fixed primary NSCLCs (stage I-IIIA) and adjacent normal lung tissue samples used for immunostaining on tissue microarrays had been obtained with informed consent from patients undergoing curative surgical operation at Hokkaido University and its affiliated hospitals (Sapporo, Japan). Histologic classification of tumors was done according to the WHO criteria (24). All tumors were staged based on the pathologic tumor-node-metastasis classification of the International Union Against Cancer (25). Postoperative staging evaluation showed that 101 patients were at stage IA, 88 at stage IB, 8 at stage IIA, 27 at stage IIB, and 43 at stage IIIA. Histopathologic examination of resected tumors revealed that 157 cases were diagnosed as adenocarcinoma, 93 cases as squamous cell carcinomas, 13 as lung large cell carcinomas, and 4 as adenosquamous carcinomas (Table 1). This study as well as the use of all clinical materials described above were approved by individual institutional Ethical Committees.

Semiquantitative reverse transcription-PCR. Total RNA was extracted from cultured cells and clinical tissues using Trizol reagent (Life Technologies, Inc., Gaithersburg, MD) according to the manufacturer's protocol. Extracted RNAs and normal human tissue polyadenylate RNAs were treated with DNase I (Nippon Gene, Tokyo, Japan) and reversely transcribed using oligo (dT) primer and SuperScript II reverse transcriptase (Invitrogen, Carlsbad, CA). Semiquantitative reverse transcription-PCR experiments were carried out with the following synthesized *IMP-1*–specific primers or with β-actin (*ACTB*)–specific primers as an internal control: *IMP-1*, 5′-CAGAAGGGACAGAGTAACCAG-3′ and 5′-GAGATCAGGGTTCCTCACTG-3′; *ACTB*, 5′-GAGGTGATAGCATTGCTTTCG-3′ and 5′-CAAGTCAGTGTACAGGTAAGC-3′. PCR reactions were optimized for the number of cycles to ensure product intensity within the logarithmic phase of amplification.

Northern blot analysis. Human multiple-tissue blots (BD Biosciences Clontech, Palo Alto, CA) were hybridized with a ^{32}P-labeled PCR

Table 1. Associations between IMP-1 expressions and clinicopathologic features in patients with lung cancer

Variables	No. cases	IMP-1 expression		*P*
		Positive (*n* = 139)	Negative (*n* = 128)	
Age (y)				
<60	84	38	46	0.1306*
≥60	183	101	82	
Gender				
Male	177	107	70	0.0001*‡
Female	90	32	58	
pT				
pT_1	117	43	74	0.0003†‡
pT_2	123	80	43	
pT_3	27	16	11	
pN				
pN_0	205	100	105	0.1639†
pN_1	26	17	9	
pN_2	36	22	14	
Histology				
ADC (including BAC)	157	57	100	<0.0001*‡
SCC	93	70	23	
LCC	13	10	3	
ASC	4	2	2	
Smoking				
Smoker	178	106	72	0.0005*‡
Nonsmoker	89	33	56	
Tumor grade				
G_1	79	27	52	0.0001*‡
Other	188	112	76	

Abbreviations: ADC, adenocarcinoma; BAC, bronchioloalveolar carcinoma; SCC, squamous cell carcinoma; LCC, large-cell carcinoma; ASC, adenosquamous carcinoma.
*χ^2 test.
†Mann-Whitney U-test.
‡Significant.

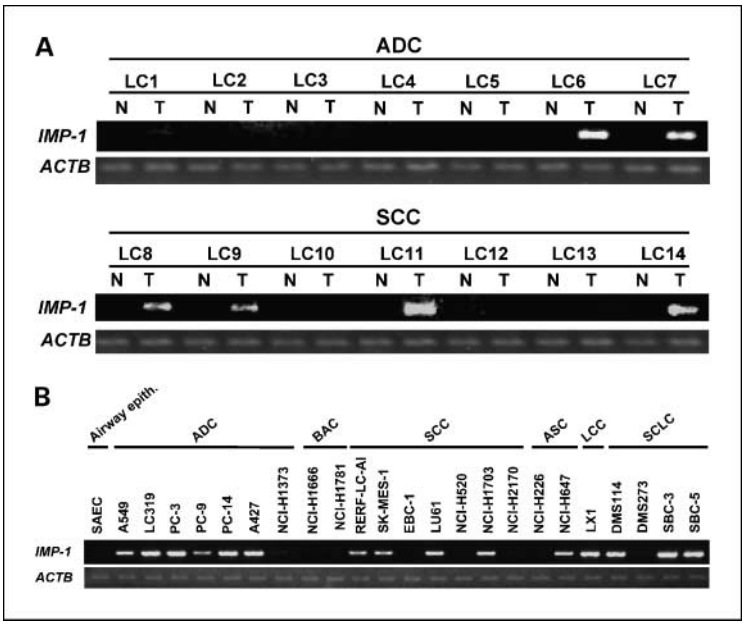

Fig. 1. Expression of *IMP-1* in lung tumors and normal tissues. *A,* expression of *IMP-1* in clinical samples of NSCLC (*T*) and corresponding normal lung tissues (*N*), examined by semiquantitative reverse transcription-PCR. Expression of *ACTB* served as a quantity control. *B,* expression of *IMP-1* transcripts in lung cancer cell lines, as revealed by semiquantitative reverse transcription-PCR.

product of *IMP-1*. The cDNA probes of *IMP-1* were prepared by reverse transcription-PCR using the primers described above. Prehybridization, hybridization, and washing were done according to the supplier's recommendations. The blots were autoradiographed at room temperature for 30 h with intensifying BAS screens (Bio-Rad, Hercules, CA).

Preparation of anti-IMP-1 polyclonal antibody. Rabbit antibodies specific for IMP-1 were raised by immunizing rabbits with IMP-1 peptides (IEHSVPKKQRSRKIC and CVKQQHQKGQSNQAQARRK) and purified using standard protocols. On Western blots, we confirmed that the antibody was specific to IMP-1 but do not cross-react with other homologous proteins (IMP-2 and IMP-3) using lysates from NSCLC cell lines transfected with IMP-1, IMP-2, and IMP-3 expressing vector and those from endogenous IMP-1 expressing/non-expressing NSCLC cells.

Western blot analysis. Cells were lysed in lysis buffer [50 mmol/L Tris-HCl (pH 8.0), 150 mmol/L NaCl, 0.5% NP40, 0.5% deoxycholate-Na, 0.1% SDS, plus protease inhibitor; Protease Inhibitor Cocktail Set III; Calbiochem, Darmstadt, Germany]. We used an enhanced chemiluminescence Western blotting analysis system (GE Healthcare Biosciences, Piscataway, NJ), as previously described (13–15). SDS-PAGE was done in 10% polyacrylamide gels. PAGE-separated proteins were electroblotted onto nitrocellulose membranes (GE Healthcare Biosciences) and incubated with a rabbit polyclonal anti-human IMP-1 antibody (1:1,000 dilution). A goat anti-rabbit IgG-horseradish peroxidase antibody (GE Healthcare Biosciences) served as the secondary antibodies for these experiments (1:10,000 dilution).

Tissue microarray construction and immunohistochemistry. Lung cancer tissue microarrays were constructed as published elsewhere, using formalin-fixed NSCLCs (12–15). Tissue areas for sampling were selected based on visual alignment with the corresponding H&E-stained sections on slides. Three, four, or five tissue cores (diameter = 0.6 mm; height = 3-4 mm) taken from donor tumor blocks were placed into recipient paraffin blocks using a tissue microarrayer (Beecher Instruments, Sun Prairie, WI). A core of normal tissue area was punched from each case. Five-micrometer sections of the resulting microarray block were used for immunohistochemical analysis.

To investigate the IMP-1 protein level in tissue microarrays of clinical samples, we stained the sections using ENVISION+ kit/horseradish peroxidase (DakoCytomation, Glostrup, Denmark). A rabbit polyclonal anti-IMP-1 antibody (1:500 dilution) was added and incubated for 1 h at room temperature after blocking endogenous peroxidase and proteins, and the sections were incubated with horseradish peroxidase–labeled anti-rabbit IgG as the secondary antibody. Substrate-chromogen was added, and the specimens were counterstained with hematoxylin. Positivity for IMP-1 was assessed semiquantitatively by three independent investigators without prior knowledge of the clinical follow-up data, each of whom recorded staining intensity as negative (scored as 0) or positive (1+). Cases were accepted as positive only if reviewers independently defined them as such.

Statistical analysis. All analyses were done using statistical analysis software (StatView, version 5.0; SAS Institute, Inc., Cary, NC). We attempted to correlate clinicopathologic variables, such as age, gender, smoking history, pathologic tumor-node-metastasis stage, histologic type, and histopathologic grading, with the expression levels of IMP-1 protein determined by tissue microarray analysis. IMP-1 immunoreactivity was assessed for association with clinicopathologic variables using the following statistical tests, such as the Mann-Whitney *U* test or χ^2 test. Multivariate logistic regression analysis was done to examine the clinicopathologic factor(s) that was independently associated with the IMP-1 expression (26, 27). Tumor-specific survival curves were calculated from the date of surgery to the time of death related to NSCLC, or to the last follow-up observation. The Kaplan-Meier method was used to generate survival curves, and survival differences were analyzed with the log-rank test, based on the status of IMP-1 expression. Univariate analysis was done using Cox's proportional hazard regression model.

RNA interference assay. We had previously established a vector-based RNA interference system (psiH1BX3.0) that was designed to synthesize small interfering RNAs (siRNA) in mammalian cells (13–15, 28). Ten micrograms of siRNA-expression vector was transfected using 30 μL LipofectAMINE 2000 (Invitrogen) into NSCLC cell lines A549 and LC319. The transfected cells were cultured for 7 days in the presence of appropriate concentrations of Geneticin (G418), and the number of colonies was counted by colony formation assay, and viability of the cells was evaluated by 3-(4,5-dimethylthiazol-2-yl)-2,5-diphenyltetrazolium bromide assay 7 days after the treatment. In 3-(4,5-dimethylthiazol-2-yl)-2,5-diphenyltetrazolium bromide assay, Cell-counting kit-8 solution (DOJINDO, Kumamoto, Japan) was added to each dish at a concentration of one-tenth volume, and the plates were incubated at 37°C for additional 4 h. Absorbance was then measured at 490 nm, and at 630 nm as a reference, with a Microplate Reader 550 (Bio-Rad). The target sequences of the synthetic oligonucleotides for RNA interference were as follows: control 1 [*enhanced green fluorescent protein* (*EGFP*) gene, a mutant of *Aequorea victoria* GFP], 5′-GAAGCAGCACGACTTCTTC-3′; control 2 (5S-16S: chloroplast *Euglena gracilis* gene coding for 5S and 16S rRNAs),

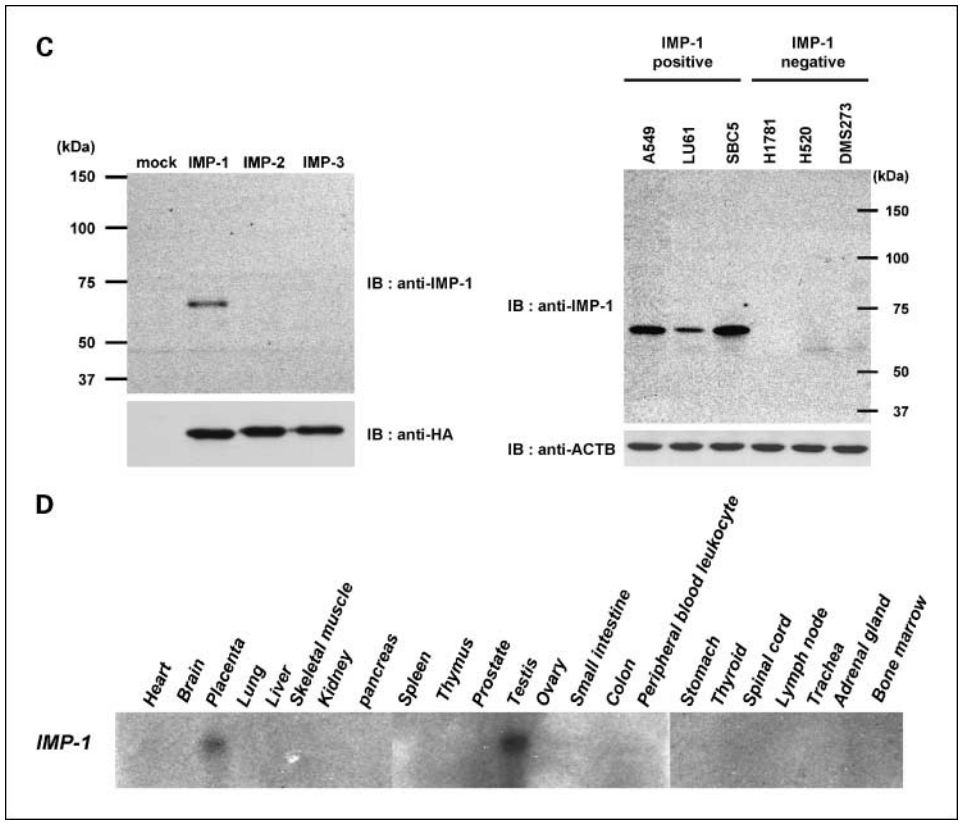

Fig. 1 *Continued. C,* specificity of anti-IMP-1 antibody displaying reaction with only IMP-1 protein, but no cross-reaction with other homologous proteins (IMP-2 and IMP-3) using lysates from NCI-H520 cells transfected with IMP-1, IMP-2, and IMP-3 expressing vector (*left*). Expression of IMP-1 protein in lung cancer cell lines by Western blot analysis (*right*). Expression of *ACTB* was as a quantity control. *D,* expression of *IMP-1* in normal human tissues, detected by Northern blot analysis.

5′-GCGCGCTTTGTAGGATTCG-3′; siRNA-*IMP-1-#1*, 5′-GCCATCAGTGTGCACTCCA-3′; siRNA-*IMP-1-#2*, 5′-GGAGGAGAACTTCTTTGGT-3′; siRNA-*IMP-1-#3*, 5′-GAATCTATGGCAAACTCAA-3′. To validate our RNA interference system, individual control siRNAs were tested by semiquantitative reverse transcription-PCR to confirm the decrease in expression of the corresponding target genes that had been transiently transfected to COS-7 cells. Down-regulation of *IMP-1* expression by functional siRNA, but not by controls, was also confirmed in the cell lines used for this assay.

Matrigel invasion assay. NIH-3T3 cells transfected either with IMP-1 constructs with NH_2-terminal FLAG- or COOH-terminal hemagglutinin-tagged sequences (pCAGGS-n3FH-IMP-1), or with mock plasmids were grown to near confluence in DMEM containing 10% FCS. The cells were harvested by trypsinization, washed in DMEM without addition of serum or proteinase inhibitor, and suspended in DMEM at concentration of 1×10^5 per mL. Before preparing the cell suspension, the dried layer of Matrigel matrix (Becton Dickinson Labware, Mountain View, CA) was rehydrated with DMEM for 2 h at room temperature. DMEM (0.75 mL) containing 10% FCS was added to each lower chamber in 24-well Matrigel invasion chambers, and 0.5 mL (5×10^4 cells) of cell suspension was added to each insert of the upper chamber. The plates of inserts were incubated for 22 h at 37°C. After incubation the chambers were processed, and cells invading through the Matrigel were fixed and stained by Giemsa as recommended by the supplier (Becton Dickinson Labware).

RNA immunoprecipitation and cDNA microarray screening for identification of IMP-1–associated mRNAs. We adopted the RNA immunoprecipitation protocol by Niranjanakumari et al. to analyze RNA(s)-protein interactions involving IMP-1 *in vivo* (29). To determine the IMP-1 associated mRNA(s), we transfected pCAGGS-n3FH-IMP-1 vector into A549 cells. Using these cell lysates transfected with IMP-1 construct, we further did immunoprecipitation experiments twice: first with monoclonal anti-FLAG M2 and then with monoclonal anti-hemagglutinin antibody. A 2.5-μg aliquot of T7-based amplified mRNA from each immunoprecipitated RNA and from the total RNA were reversely transcribed in the presence of Cy5-dCTP and Cy3-dCTP, respectively, as described previously (9–11), for hybridization to a cDNA microarray representing 27,648 genes (IP-microarray analysis).

Results

Expression of IMP-1 transcripts in lung tumors and normal tissues. To identify target molecules for development of novel therapeutic agents and/or biomarkers for lung cancer, we first screened a cDNA microarray for genes that showed ≥3-fold expression in >50% of NSCLCs analyzed (9, 10). Among 27,648 genes screened, we identified the *IMP-1* transcript to show >3-fold expression in 68.8% of NSCLCs compared with normal lung tissue (control). We confirmed its overexpression by semiquantitative reverse transcription-PCR experiments in 6 of 14 additional NSCLC cases (2 of 7 adenocarcinomas and 4 of 7 squamous cell carcinomas; Fig. 1A) as well as in 16 of 23 NSCLC and SCLC cell lines. However, its expression was hardly detectable in small airway epithelial cells derived from normal bronchial epithelium (Fig. 1B).

We subsequently generated rabbit polyclonal antibody against human IMP-1 and confirmed its specificity to IMP-1 by Western blot analysis that showed no cross-reactivity to other homologous proteins (IMP-2 and IMP-3) using lysate from NCI-H520 cells that had been transfected with hemagglutinin-tagged IMP-1, IMP-2, or IMP-3 expression vector (Fig. 1C, *left*). Using this antibody, we confirmed expression of endogenous IMP-1 protein in six lung cancer cell lines by Western blot analysis (three IMP-1–positive and three IMP-1–negative cell

lines; Fig. 1C, *right*). Northern blot analysis using *IMP-1* cDNA as a probe identified strong signals corresponding to 4.5-kb transcript that expressed specifically in placenta and testis (Fig. 1D).

Association of IMP-1 expression with poor prognosis of NSCLC patients. To verify the clinicopathologic significance of IMP-1, we additionally examined the expression of IMP-1 protein by means of tissue microarrays containing lung cancer tissues from 267 patients. Positive tumor cells generally showed a cytoplasmic staining pattern in NSCLC, and no staining was observed in any of their adjacent normal lung tissues (Fig. 2A). We classified patterns of IMP-1 expression as negative (scored as 0) or positive (scored as 1+; Fig. 2A). We found positive staining in 139 (52.1%) of 267 NSCLC cases; 57 of 157 adenocarcinoma tumors (36.3%), 70 of 93 squamous cell carcinoma tumors (75.3%), 10 of 13 lung large cell carcinoma tumors (76.9%), and 2 of 4 adenosquamous carcinoma tumors (50.0%) were judged to be positive (Table 1). We then examined a correlation of IMP-1 expression with various clinicopathologic variables and found its significant correlation with gender (higher in male, $P = 0.0001$), pT classification (higher in larger tumor, $P = 0.0003$), histopathologic type (higher in non-adenocarcinoma, $P < 0.0001$), smoking history (higher in smoker, $P = 0.0005$), and histopathologic grade (higher in non–well-differentiated tumor, $P = 0.0001$; Table 1). Multivariate logistic regression analysis for these five significant clinicopathologic variables determined that larger tumor size (pT_2-T_3), non-adenocarcinoma histology, and non–well-differentiated histopathologic grade were independent features associated with IMP-1 overexpression ($P = 0.0104$, 0.0001, and 0.0019, respectively; Supplementary Table S1).

The Kaplan-Meier analysis indicated a significant association between IMP-1 positivity in NSCLCs and tumor-specific 5-year survival ($P = 0.0053$ by the log-rank test; Fig. 2B). By univariate analysis using the Cox proportional hazard model, gender (male versus female), pT (T_2-T_4 versus T_1), pN (N_1-N_2 versus N_0), N_0), histologic type (non-adenocarcinoma versus adenocarcinoma), smoking history (smoker versus nonsmoker), and IMP-1 expression (positive versus negative) were all significantly related to poor tumor-specific survival among NSCLC patients ($P = 0.0286$, <0.0001, <0.0001, 0.0003, 0.0220, and 0.0064, respectively; Table 2).

Growth inhibition of NSCLC cells by specific siRNA against IMP-1. To assess whether *IMP-1* is essential for growth or survival of lung-cancer cells, we constructed plasmids to express

Table 2. Prognostic factors in Cox proportional hazards model

Variables	Risk ratio (univariate 95% confidence interval)	*P*
Age (y)		
≥60/<60	1.686 (0.963-2.954)	0.0677
Sex		
Male/female	1.848 (1.066-3.205)	0.0286*
pT		
pT_2-T_4/pT_1	3.145 (1.789-5.525)	<0.0001*
pN		
pN_1-N_2/pN_0	4.310 (2.660-6.993)	<0.0001*
Histologic type		
Non-ADC/ADC	2.463 (1.508-4.016)	0.0003*
Histopathologic grade		
Other/G_1	1.072 (0.645-1.783)	0.7879
Smoking		
Smoker/nonsmoker	1.883 (1.095-3.236)	0.0220*
IMP-1 expression		
Positive/negative	2.045 (1.224-3.425)	0.0064*

Abbreviation: ADC, adenocarcinoma.
*Significant.

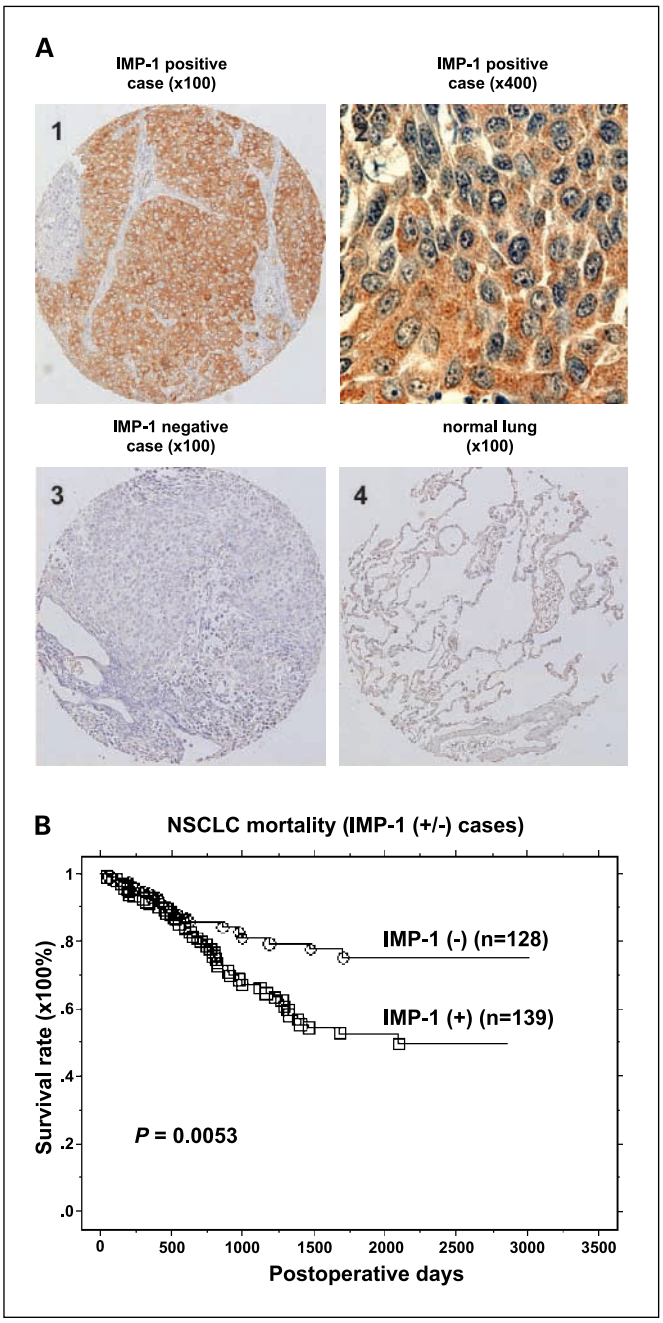

Fig. 2. Association of IMP-1 overexpression with poor prognosis of NSCLC patients. *A,* representative example of positive or negative expression of IMP-1 in lung cancer (squamous cell carcinomas; ×100 and ×400) and normal lung (×100). Detection of IMP-1 protein by immunohistochemistry using the rabbit polyclonal anti-IMP-1 antibody. Counterstaining with hematoxylin. *B,* Kaplan-Meier analysis of tumor specific survival in NSCLC patients according to IMP-1 expression level.

siRNAs against IMP-1 (si-*IMP-#1*, si-*IMP-#2*, and si-*IMP-#3*) and control plasmids (siRNAs for EGFP and 5S-16S) and transfected them into lung cancer cell lines A549 and LC319. The mRNA levels in cells transfected with si-*IMP-1-#2* or si-*IMP-1-#3* were significantly decreased in comparison with cells transfected with either control siRNAs or si-*IMP-1-#1*. We observed significant decreases in the number of colonies and in the numbers of viable cells measured by 3-(4,5-dimethylthiazol-2-yl)-2,5-diphenyltetrazolium bromide assay, suggesting that up-regulation of IMP-1 is related to growth or survival of cancer cells (representative data of A549 were shown in Fig. 3A and B).

Activation of cellular migration by IMP-1. As the immunohistochemical analysis on tissue microarray had indicated that NSCLC patients with IMP-1–positive tumors showed shorter cancer-specific survival periods than those with IMP-1–negative tumors, we examined a possible role of IMP-1 in cell migration and invasion using Matrigel assays, using NIH-3T3 cells. As shown in Fig. 3C, transfection of IMP-1 cDNA into NIH-3T3 cells significantly enhanced its invasive ability through Matrigel, compared with those transfected with mock vector.

Isolation of mRNAs associated with IMP-1 using RNA immunoprecipitation and cDNA microarray. IMP-1 protein is known to exhibit attachments to at least four RNAs (30). IMP-1 binds specifically to (*a*) one of the two *cis*-acting, c-*myc* mRNA instability elements (31); (*b*) the 5′-untranslated region of the leader-3 *IGF-II* mRNA, which represents the major embryonic form of this message (17); (*c*) the *H19* RNA, a gene product exhibiting an oncofetal pattern of expression (23); and (*d*) the neuron-specific *tau* mRNA that encodes a microtubule-associated protein localized primarily in the cell body and axon of developing neurons (32). However, expression pattern of these mRNAs in lung cancers we examined were not necessarily concordant with that of IMP-1 (data not shown). Therefore, to elucidate the function of IMP-1 in pulmonary carcinogenesis, we searched for another candidate mRNA(s) that would interact with IMP-1 and might thereby play important roles in growth and/or progression of lung cancer using RNA immunoprecipitation and cDNA microarray (IP-microarray). First, we co-hybridized Cy5-labeled mRNAs that were immunoprecipitated with IMP-1 (IP-mRNA) and Cy3-labeled total RNAs isolated from A549 cells on cDNA microarrays. Then, to identify the up-regulated genes in A549 cells compared with normal lung tissues, we co-hybridized with Cy5-labeled total RNAs isolated from A549 cells and Cy3-labeled polyadenylate RNAs derived from normal lung (Clontech). Among 27,648 genes screened, we identified a total of 22 transcripts that were both enriched in IMP-1-IP-mRNA(s) (>2-fold intensity)

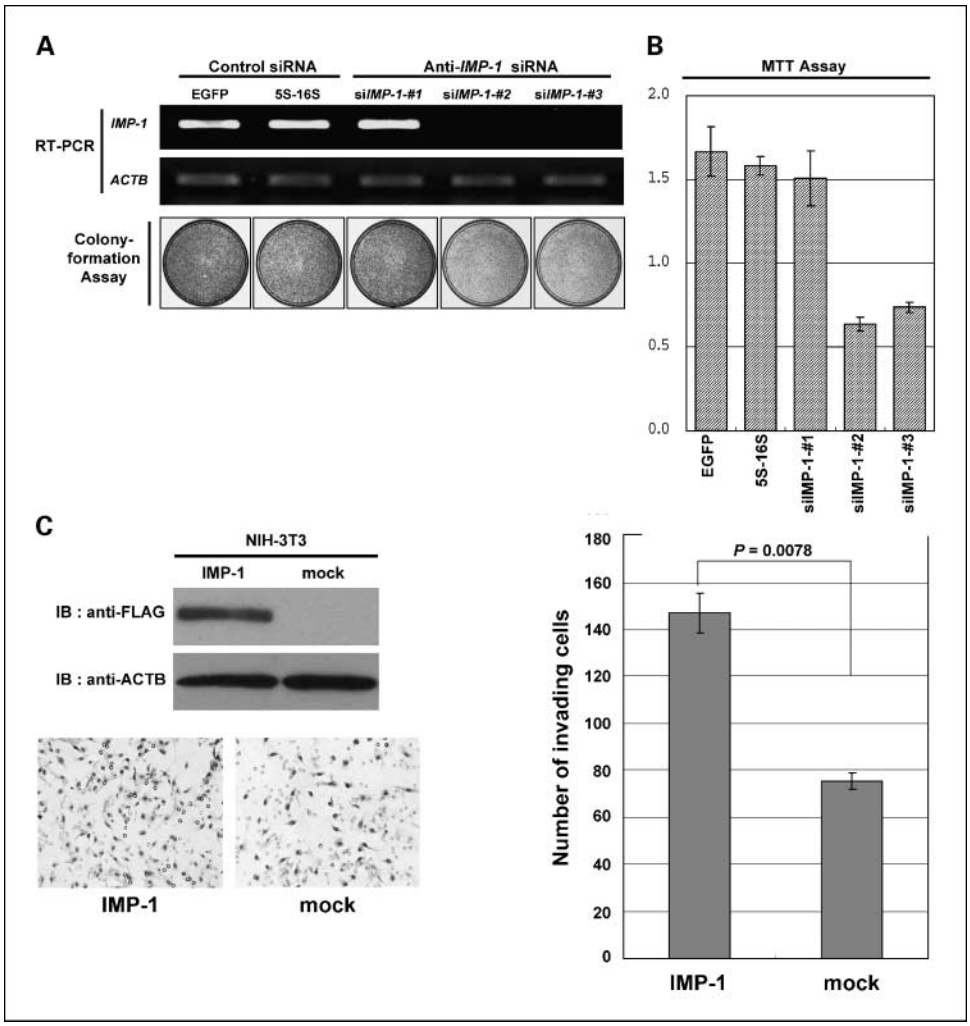

Fig. 3. Inhibition of growth of NSCLC cells by siRNA against *IMP-1* and activation of cellular motility/invasion by IMP-1. *A,* response of A549 cells to si-*IMP-1* or control siRNAs (si-EGFP or si-5S-16S). Top, level of *IMP-1* expression detected by semiquantitative reverse transcription-PCR in cells treated with either control or si-*IMP-1s*. Bottom, colony formation assays using A549 cells transfected with siRNA to *IMP-1* (*#1-#3*). *B,* effect of siRNA against *IMP-1* on cell viability, detected by 3-(4,5-dimethylthiazol-2-yl)-2,5-diphenyltetrazolium bromide assays. *C,* assays showing the invasive nature of NIH-3T3 cells in Matrigel matrix after transfection with plasmids designed to express human IMP-1. Left, (*top*) transient expression of IMP-1 in NIH-3T3 cells, detected by Western blot analysis. Bottom, Giemsa staining (×200) and (*right*) the number of cells migrating through the Matrigel-coated filters. Assays were done thrice, each in triplicate wells.

Table 3. List of 22 candidate mRNAs associated with the IMP-1 identified using RNA immunoprecipitation and cDNA microarray

Rank*	Accession	Hs.ID	Gene name	Title	Ratio† of IP-mRNA by IMP-1/total RNA in A549	Relative gene expression‡ (A549/lung)
1	U68019	549051	*SMAD3*	SMAD, mothers against DPP homologue 3 (*Drosophila*)	720.08	2.66
2	CA427461	10842	*RAN*	RAN, member RAS oncogene family	81.86	3.21
3	NM_004939	440599	*DDX1*	DEAD (Asp-Glu-Ala-Asp) box polypeptide 1	34.19	2.66
4	NM_004209	435277	*SYNGR3*	Synaptogyrin 3	12.32	12.93
5	BM683457	73962	*EPHA7*	EPH receptor A7	10.04	2.77
6	U05569	184085	*CRYAA*	Crystallin, alpha A	9.77	2.17
7	BC050284	11747	*YTHDF1*	YTH domain family, member 1	7.99	2.20
8	M91670	396393	*UBE2S*	Ubiquitin-conjugating enzyme E2S	6.78	6.42
9	AY454159	121520	*AMIGO2*	Adhesion molecule with immunoglobulin-like domain 2	5.65	18.09
10	AA112466	554875	*PDF*	Peptide deformylase-like protein	4.18	3.93
11	AI076810	133977	*MGC27277*	Chromosome 1 open reading frame 67	3.43	136.99
12	AI242497	151675	*C20orf142*	Chromosome 20 open reading frame 142	3.21	3.79
13	NM_032438	486466	*L3MBTL3*	L(3)mbt-like 3 (Drosophila)	3.19	3.12
14	D86960	497674	*LPGAT1*	Lysophosphatidylglycerol acyltransferase 1	3.14	7.84
15	NM_003463	227777	*PTP4A1*	Protein tyrosine phosphatase type IVA, member 1	3.00	2.02
16	BC007560	334851	*LASP1*	LIM and SH3 protein 1	2.66	2.86
17	NM_024052	187422	*C17orf39*	Chromosome 17 open reading frame 39	2.57	2.77
18	AA191573	434494	*SYNJ2*	Synaptojanin 2	2.56	4.33
19	X04217	82609	*HMBS*	Hydroxymethylbilane synthase	2.48	2.15
20	NM_007007	369606	*CPSF6*	Cleavage and polyadenylation-specific factor 6, 68kDa	2.24	3.02
21	U97188	432616	*IMP-3*	IGF-II mRNA-binding protein 3	2.09	34.00
22	NM_019592	168095	*RNF20*	Ring finger protein 20	2.01	2.52

*Probe sets are ranked by the ratio (IMP-1 IP-mRNAs/total RNAs in A549 cells).
†Ratios [mRNAs that were immunoprecipitated from A549 lysates with IMP-1 (IP-mRNA)/total RNAs isolated from A549 cells].
‡Ratios (gene expression levels in A549 cells compared with normal lung tissues).

and overexpressed (>2-fold intensity) in A549 cell line compared with normal lung (Table 3). The 22 genes represented a variety of functions, including genes involved in signal transduction (*SMAD3* and *RAN*), cell adhesion and cytoskeleton (*AMIGO2* and *LASP1*), ubiquitination (*UBE2S* and *RNF20*), and some phosphatases (*PTP4A1* and *SYNJ2*; refs. 33–39). Several of them have been indicated to have important roles in carcinogenesis (e.g., involvement of *AMIGO2 LASP1*, *SYNJ2*, and *PTP4A1* in cell invasion and migration; refs. 34, 35, 38, 39).

Discussion

ACTB mRNA is transported to the leading lamellae of chicken embryo fibroblasts and to the growth cones of developing neurons (40, 41). The localization of *ACTB* mRNA depends on the "zipcode," a *cis*-acting element in the 3′ untranslated region of the mRNA (42). The respective *trans*-acting factor, zipcode-binding protein 1, was identified by affinity purification with the zipcode of *ACTB* mRNA, and it seems to shuttle this RNA to the leading edge of migrating cells (43). Homologues of zipcode-binding protein 1 have since been identified in a wide range of organisms, including frog, fly, mouse, and human (44–46). Zipcode-binding protein 1–like proteins contain two RNA recognition motifs in the NH_2-terminal region and four ribonucleoprotein K homology domains at the COOH-terminal end. IMP-1, one of the *IGF2* mRNA-binding proteins, is considered a member of the zipcode-binding protein 1 family. It exhibits multiple attachments to *IGF2* leader-3 mRNA and is overexpressed in several human cancers (18–21). In this study, we confirmed by siRNA and cell invasion experiments that IMP-1 could play a significant role in the tumor cell growth/survival and tumor progression. Furthermore, we undertook RNA immunoprecipitation experiments coupled with cDNA microarrays (IP-microarray) and identified dozens of candidate mRNAs that were likely to be associated with IMP-1 in NSCLC cells (see Table 3). The list included many genes encoding proteins functioning in signal transduction, cell adhesion and cytoskeleton, and those having various types of enzymatic activities. For example, *RAN* (ras-related nuclear protein) is a small GTP-binding protein belonging to the RAS superfamily that is essential for the translocation of RNA and proteins through the nuclear pore complex (47). Ran system is deregulated in certain cellular contexts: this may represent a favoring condition for the onset and propagation of mitotic errors that can predispose cells to become genetically unstable and facilitate neoplastic growth (48).

Intracellular mRNA transport by RNA-binding proteins has been reported in oocytes and developing embryos of fly and frog and in somatic cells, such as fibroblasts and neurons (49, 50). IMP-1, which is expressed only in cancers and limited normal tissues, such as placenta, testis, and fetal tissues, may be required for the transport of certain mRNAs that play essential roles in embryogenesis and carcinogenesis. Interestingly, induction of exogenous IMP-1 expression into A549 cells did not change the levels of proteins encoded by the IMP-1–associated mRNAs (we used antibodies to EPHA7 and IMP-3 listed in Table 3 for Western blotting; data not

shown), indicating that the IMP-1 binding to the various mRNAs is unlikely to affect their protein levels. Therefore, it is rather speculated that proliferating germ cells or cancer cells may actively distribute indispensable mRNAs in cells through the transporting system involved in the IMP-1 protein-mRNA complex. The evidence that IMP-1 associates with various mRNAs encoding proteins involved in cell cycle progression, cell invasion and migration, and various types of enzymatic activities supports that hypothesis. In fact, IMP-1 positivity was correlated with tumor extension factor (pT classification) by clinicopathologic investigation using tissue microarray. Further investigations of IMP-1–associated mRNAs could lead to a better understanding of the development of NSCLCs.

We also showed that IMP-1 is expressed significantly higher in lung cancer cells than normal lung cells. Copy number gains at the *IMP-1* loci (*17q21*) were observed in 18.3% of primary breast cancers (19). To elucidate the mechanism of IMP-1 overexpression, we examined gene amplification of *IMP-1* by semiquantitative genomic PCR analysis of a couple of lung cancer materials, but we found no amplification of the *IMP-1* loci in these cases (data not shown), implying that *IMP-1* overexpression should be not regulated by genetic alterations but by epigenetic mechanisms. We also found that IMP-1 might play an important role in the development/progression of lung cancers. In particular, our results showed that IMP-1 overexpression is associated with lung cancer progression, resulting in a poor prognosis for patients with lung cancer. Concordantly, induction of exogenous expression of IMP-1 enhanced the cellular migration/invasive activity of mammalian cells. IMP-1 overexpression in resected specimens may be a useful index for application of adjuvant therapy to the patients who are likely to have poor prognosis. Furthermore, our data indicated that upregulation of IMP-1 is related to growth or survival of cancer cells. Although the molecular mechanisms underlying increased IMP-1 expression levels in many cancer cells have not been elucidated, IMP-1 may represent a promising molecular target for human cancer treatment.

References

1. Greenlee RT, Hill-Harmon MB, Murray T, Thun M. Cancer statistics, 2001. CA Cancer J Clin 2001;51:15–36.
2. Sozzi G. Molecular biology of lung cancer. Eur J Cancer 2001;37 Suppl 7:S63–73.
3. Schiller JH, Harrington D, Belani CP, et al. Comparison of four chemotherapy regimens for advanced non-small-cell lung cancer. N Engl J Med 2002;346:92–8.
4. Kelly K, Crowley J, Bunn PA, Jr., et al. Randomized phase III trial of paclitaxel plus carboplatin versus vinorelbine plus cisplatin in the treatment of patients with advanced non-small-cell lung cancer: a Southwest Oncology Group trial. J Clin Oncol 2001;19:3210–8.
5. Lynch TJ, Bell DW, Sordella R, et al. Activating mutations in the epidermal growth factor receptor underlying responsiveness of non-small-cell lung cancer to gefitinib. N Engl J Med 2004;350:2129–39.
6. Paez JG, Janne PA, Lee JC, et al. EGFR mutations in lung cancer: correlation with clinical response to gefitinib therapy. Science 2004;304:1497–500.
7. Tsao MS, Sakurada A, Cutz JC, et al. Erlotinib in lung cancer: molecular and clinical predictors of outcome. N Engl J Med 2005;353:133–44.
8. Shepherd FA, Rodrigues Pereira J, Ciuleanu T, et al. Erlotinib in previously treated non-small-cell lung cancer. N Engl J Med 2005;353:123–32.
9. Kikuchi T, Daigo Y, Katagiri T, et al. Expression profiles of non-small cell lung cancers on cDNA microarrays: identification of genes for prediction of lymph-node metastasis and sensitivity to anti-cancer drugs. Oncogene 2003;22:2192–205.
10. Kakiuchi S, Daigo Y, Ishikawa N, et al. Prediction of sensitivity of advanced non-small cell lung cancers to gefitinib (Iressa, ZD1839). Hum Mol Genet 2004;13:3029–43.
11. Taniwaki M, Daigo Y, Ishikawa N, et al. Increases of amphiregulin and transforming growth factor-alpha in serum as predictors of poor response to gefitinib among patients with advanced non-small cell lung cancers. Int J Oncol 2005;65:9176–84.
12. Ishikawa N, Daigo Y, Yasui W, et al. ADAM8 as a novel serological and histochemical marker for lung cancer. Clin Cancer Res 2004;10:8363–70.
13. Kato T, Daigo Y, Hayama S, et al. A novel human tRNA-dihydrouridine synthase involved in pulmonary carcinogenesis. Cancer Res 2005;65:5638–46.
14. Furukawa C, Daigo Y, Ishikawa N, et al. Plakophilin 3 oncogene as prognostic marker and therapeutic target for lung cancer. Cancer Res 2005;65:7102–10.
15. Suzuki C, Daigo Y, Ishikawa N, et al. ANLN plays a critical role in human lung carcinogenesis through the activation of RHOA and by involvement in the phosphoinositide 3-kinase/AKT pathway. Cancer Res 2005;65:11314–25.
16. Nielsen J, Adolph SK, Rajpert-De Meyts E, et al. Nuclear transit of human zipcode-binding protein IMP1. Biochem J 2003;376:383–91.
17. Nielsen J, Christiansen J, Lykke-Andersen J, et al. A family of insulin-like growth factor II mRNA-binding proteins represses translation in late development. Mol Cell Biol 1999;19:1262–70.
18. Ross J, Lemm I, Berberet B. Overexpression of an mRNA-binding protein in human colorectal cancer. Oncogene 2001;20:6544–50.
19. Ioannidis P, Mahaira L, Papadopoulou A, et al. 8q24 Copy number gains and expression of the c-*myc* mRNA stabilizing protein CRD-BP in primary breast carcinomas. Int J Cancer 2003;104:54–9.
20. Ioannidis P, Kottaridi C, Dimitriadis E, et al. Expression of the RNA-binding protein CRD-BP in brain and non-small cell lung tumors. Cancer Lett 2004;209:245–50.
21. Gu L, Shigemasa K, Ohama K. Increased expression of IGF II mRNA-binding protein 1 mRNA is associated with an advanced clinical stage and poor prognosis in patients with ovarian cancer. Int J Oncol 2004;24:671–8.
22. Nielsen FC, Nielsen J, Kristensen MA, Koch G, Christiansen J. Cytoplasmic trafficking of IGF-II mRNA-binding protein by conserved KH domains. J Cell Sci 2002;115:2087–97.
23. Runge S, Nielsen FC, Nielsen J, et al. H19 RNA binds four molecules of insulin-like growth factor II mRNA-binding protein. J Biol Chem 2000;275:29562–9.
24. WHO. International histological classification of tumours. 3rd ed. Genova: WHO; 1999.
25. Sobin L, Wittekind Ch. TNM classification of malignant tumours. 6th ed. New York: Wiley-Liss, Inc.; 2002.
26. Mishina T, Dosaka-Akita H, Hommura F, et al. Cyclin E expression, a potential prognostic marker for non-small cell lung cancers. Clin Cancer Res 2000;6:11–6.
27. Hommura F, Dosaka-Akita H, Mishina T, et al. Prognostic significance of p27KIP1 protein and ki-67 growth fraction in non-small cell lung cancers. Clin Cancer Res 2000;6:4073–81.
28. Suzuki C, Daigo Y, Kikuchi T, Katagiri T, Nakamura Y. Identification of COX17 as a therapeutic target for non-small cell lung cancer. Cancer Res 2003;63:7038–41.
29. Niranjanakumari S, Lasda E, Brazas R, Garcia-Blanco MA. Reversible cross-linking combined with immunoprecipitation to study RNA-protein interactions *in vivo*. Methods 2002;26:182–90.
30. Ioannidis P, Mahaira LG, Perez SA, et al. CRD-BP/IMP1 expression characterizes cord blood $CD34^+$ stem cells and affects c-myc and IGF-II expression in MCF-7 cancer cells. J Biol Chem 2005;280:20086–93.
31. Bernstein PL, Herrick DJ, Prokipcak RD, Ross J. Control of c-*myc* mRNA half-life *in vitro* by a protein capable of binding to a coding region stability determinant. Genes Dev 1992;6:642–54.
32. Atlas R, Behar L, Elliott E, Ginzburg I. The insulin-like growth factor mRNA binding-protein IMP-1 and the Ras-regulatory protein G3BP associate with tau mRNA and HuD protein in differentiated P19 neuronal cells. J Neurochem 2004;89:613–26.
33. Kurisaki A, Kurisaki K, Kowanetz M, et al. The mechanism of nuclear export of Smad3 involves exportin 4 and Ran. Mol Cell Biol 2006;26:1318–32.
34. Rabenau KE, O'Toole JM, Bassi R, et al. DEGA/AMIGO-2, a leucine-rich repeat family member, differentially expressed in human gastric adenocarcinoma: effects on ploidy, chromosomal stability, cell adhesion/migration and tumorigenicity. Oncogene 2004;23:5056–67.
35. Strehl S, Borkhardt A, Slany R, et al. The human LASP1 gene is fused to MLL in an acute myeloid leukemia with t(11;17)(q23;q21). Oncogene 2003;22:157–60.
36. Liu Z, Diaz LA, Haas AL, Giudice GJ. cDNA cloning of a novel human ubiquitin carrier protein. An antigenic domain specifically recognized by endemic pemphigus foliaceus autoantibodies is encoded in a secondary reading frame of this human epidermal transcript. J Biol Chem 1992;267:15829–35.
37. Zhu B, Zheng Y, Pham AD, et al. Monoubiquitination of human histone H2B: the factors involved and their roles in HOX gene regulation. Mol Cell 2005;20:601–11.
38. Stephens BJ, Han H, Gokhale V, Von Hoff DD. PRL phosphatases as potential molecular targets in cancer. Mol Cancer Ther 2005;4:1653–61.
39. Chuang YY, Tran NL, Rusk N, et al. Role of synaptojanin 2 in glioma cell migration and invasion. Cancer Res 2004;64:8271–5.
40. Lawrence JB, Singer RH. Intracellular localization of messenger RNAs for cytoskeletal proteins. Cell 1986;45:407–15.
41. Bassell GJ, Zhang H, Byrd AL, et al. Sorting of beta-actin mRNA and protein to neurites and growth cones in culture. J Neurosci 1998;18:251–65.

42. Kislauskis EH, Li Z, Singer RH, Taneja KL. Isoform-specific 3′-untranslated sequences sort alpha-cardiac and beta-cytoplasmic actin messenger RNAs to different cytoplasmic compartments. J Cell Biol 1993;123:165–72.

43. Ross AF, Oleynikov Y, Kislauskis EH, Taneja KL, Singer RH. Characterization of a beta-actin mRNA zipcode-binding protein. Mol Cell Biol 1997;17:2158–65.

44. Mueller-Pillasch F, Lacher U, Wallrapp C, et al. Cloning of a gene highly overexpressed in cancer coding for a novel KH-domain containing protein. Oncogene 1997;14:2729–33.

45. Deshler JO, Highett MI, Schnapp BJ. Localization of *Xenopus* Vg1 mRNA by Vera protein and the endoplasmic reticulum. Science 1997;276:1128–31.

46. Doyle GA, Betz NA, Leeds PF, et al. The c-myc coding region determinant-binding protein: a member of a family of KH domain RNA-binding proteins. Nucleic Acids Res 1998;26:5036–44.

47. Yokoyama N, Hayashi N, Seki T, et al. A giant nucleopore protein that binds Ran/TC4. Nature 1995;376:184–8.

48. Di Fiore B, Ciciarello M, Lavia P. Mitotic functions of the Ran GTPase network: the importance of being in the right place at the right time. Cell Cycle 2004;3:305–13.

49. King ML, Zhou Y, Bubunenko M. Polarizing genetic information in the egg: RNA localization in the frog oocyte. Bioessays 1999;21:546–57.

50. Mowry KL, Cote CA. RNA sorting in *Xenopus* oocytes and embryos. FASEB J 1999;13:435–45.